Cancer Science
The official journal of the Japanese Cancer Association

Decreased expression of germinal center–associated nuclear protein is involved in chromosomal instability in malignant gliomas

Kazutaka Ohta,[1,2] Kazuhiko Kuwahara,[1] Zhenhuan Zhang,[1] Keishi Makino,[2] Yoshihiro Komohara,[3] Hideo Nakamura,[2] Jun-ichi Kuratsu[2] and Nobuo Sakaguchi[1,4,5]

Departments of [1]Immunology, [2]Neurosurgery and [3]Cell Pathology, Graduate School of Medical Sciences, Kumamoto University, Kumamoto; [4]CREST, Japan Science and Technology Agency (JST), Japan

(Received May 29, 2009/Revised July 09, 2009/Accepted July 12, 2009/Online publication August 16, 2009)

Malignant glioma (MG) is highly proliferative and invasive, with the malignant characteristics associated with aneuploidy and chromosomal instability (CIN). Here, we found that the level of germinal center–associated nuclear protein (GANP), a mammalian homologue of yeast Sac3, was markedly decreased in MGs with a poor prognosis; and thus we explored the effect of its decrease on cell-cycle progression of MG cell lines. Glioblastomas showed a significantly lower level of *ganp* mRNA than anaplastic astrocytomas, as measured by real-time reverse transcription-PCR, in 101 cases of adult MG. MGs of *ganp*^{Low} expression displayed more malignant characteristics, with loss of heterozygosity on chromosome 10, epidermal growth factor receptor gene amplification, and significantly poorer prognosis than the *ganp*^{High} group. Human diploid fibroblasts depleted of *ganp* mRNA by the RNA interference (RNAi) method showed a decreased percentage of S-phase cells and a cellular-senescence phenotype. MG cell lines harboring abnormalities of various cell-cycle checkpoint molecules displayed slippage of mitotic checkpoints and an increased proportion of hyperploid cells after *ganp* RNAi-treatment. These results suggest that GANP protects cells from cellular senescence caused by DNA damage and that a significant decrease in GANP expression leads to malignancy by generating hyperploidy and CIN. (*Cancer Sci* 2009; 100: 2069–2076)

Human malignant gliomas (MGs), diagnosed as anaplastic astrocytoma (AA) and glioblastoma multiforme (GBM), are composed of different cell types displaying a wide spectrum of heterogeneity regarding morphology, biological aggressiveness, invasive potentiality, and treatment sensitivity.[1] Extensive genetic studies have shown that MGs reveal distinctive features of complex chromosome aberrations, resulting in the loss of heterozygosity of the chromosomes carrying tumor suppressors of PTEN and p16/Cdkn2/Ink4, and in the amplification of epidermal growth factor receptor (EGFR) and human double minute-2 oncoprotein (HDM2).[2–5] Chromosomal instability (CIN), appearing as chromosome gains or losses, occurs frequently during the cell-cycle processes of DNA synthesis, chromosomal duplication and segregation, and cytokinesis[6] as a result of various kinds of DNA damage. A sensor mechanism in cells initially recognizes DNA damage as single-stranded DNA breaks or double-stranded DNA breaks (DSBs) and then induces a DNA damage response (DDR) acting through either a cellular-senescence mechanism that keeps the damaged cells proliferation silent at cell-cycle checkpoints or an apoptotic mechanism that eliminates the DNA-damaged cells.[7]

Accumulated evidence has demonstrated that DNA damage occurs to genes during active gene transcription as transcription-coupled DNA damage during the G1-phase[8] in a yeast model that lacks mRNA export molecules.[9] The molecular mechanisms of mRNA export have been intensively studied by using yeast cells.[10,11] The yeast Sac3 protein is associated with Thp1 protein as a Sac3/Thp1 complex that is necessary for the transport of ribonucleoprotein complexes bound to SAGA complexes to the nuclear pore and toward the cytoplasm.[12] The lack of either one of these components causes homology-mediated DNA hyper-recombination at a high frequency that is measured by an artificial reporter construct of tandem-repeat *leu2* gene.

A mammalian homologue of Sac3 was identified as germinal center–associated nuclear protein (GANP), which is a protein required for affinity maturation of antigen-stimulated B-cells.[13–15] GANP contains two functional domains potentially involved in DNA replication: the NH_2-terminal RNA-primase domain[16] and the COOH-terminal MCM3-binding/acetylating domain.[17] Overexpression of *ganp* cDNA in Daudi B-cells causes DNA synthesis to exceed that in the mock-transfectants.[16] Transgenic mice (*ganp*-Tg) that express the *ganp* transgene in B lineage cells show a high incidence of lymphomagenesis (29.5%) after they have aged.[18] The middle region of GANP is homologous to Sac3, implying that GANP might be involved in the mRNA export complex. The introduction of *ganp* into NIH-3T3 cells suppressed homology-mediated DNA hyper-recombination caused by DSBs after restriction enzyme digestion with *I-sce*I, and this activity was restricted to the Sac3-homology region of GANP.[19] In mammals, however, there are few studies providing evidence for the involvement of GANP in mRNA export and none indicating its association with transcription-coupled DNA damage and cancer cells in clinical cases. Here, we examined whether an abnormality in GANP related to the export of mRNA complexes exists in clinical cancer cases by focusing on various malignant neoplasm originating in the central nervous system (CNS). GANP expression was significantly decreased in MGs with poor prognosis. Remarkably, a decrease in GANP expression caused the accumulation of senescence-phenotype cells among human diploid fibroblast cells, presumably indicating that GANP expression is normally essential to suppress DNA damage during cell culture. GANP insufficiency was associated with the induction of CIN in the cells harboring various genetic abnormalities in their cell cycle and checkpoints, indicating that a decrease in GANP expression is a critical factor for the progression of malignancy in gliomas.

Materials and Methods

Patients and samples. Samples were obtained from the Department of Neurosurgery at Kumamoto University Hospital. The 101 patients were from a consecutive series, and no

[5]To whom correspondence should be addressed.
E-mail: nobusaka@gpo.kumamoto-u.ac.jp

doi: 10.1111/j.1349-7006.2009.01293.x

Table 1. Primer sequences

Primer name	Forward (5′–3′)	Reverse (5′–3′)
siRNA		
ganp siRNA	CCAGCGUCUUCUGGAGUAAGUCAUU	AAUGACUUACUCCAGAAGACGCUGG
ganp siRNA2	CCCAAACCUCAAGUGUUGGACCCUU	AAGGGUCCAACACUUGAGGUUUGGG
scrambled control siRNA	CCCACCUCAAGUGUUGGACCAACUU	AAGUUGGUCCAACACUUGAGGUGGG
Real-time RT-PCR		
ganp	CGTGGAGCTGATGGAACG	GCAGAAGCACTGAAGCTCCT
ganp donor probe	AGTGGGCACAGACATCCTCACAGCAACG	—
ganp acceptor probe	GCCACACGGACCCTCTGGTCTGTCTCTA	—
gapdh	CAGCCTCAAGATCATCAGC	GGCCATCCACAGTCTTCT
gapdh donor probe	GGTCATCCATGACAACTTTGGTATCATGGAA	—
gapdh acceptor probe	GACTCATGACCACAGTCCATGCCATCACTG	—

exclusion criteria were applied. RNA extraction from samples and reverse transcription (RT) reaction were performed.[20] The patients and/or their legal guardians gave written informed consent for use of their specimens. Median age of the patients was 51 years (range, 17–78 years). All patients underwent surgical resection (including biopsy) with or without postoperative radiotherapy and/or nitrosourea-based chemotherapy. GBM patients younger than 70 years of age received both radiotherapy and chemotherapy; older patients usually received radiotherapy only. Clinical details, date of recurrence (or regrowth) on magnetic resonance imaging, and date of death were recorded. The survival time was measured as the time from the date of the initial surgery to the date of death or to the date of analysis (1 June 2007). Progression-free survival time was measured from the date of initial surgery to the onset of clinical deterioration or the tumor recurrence confirmed radiologically. MIB-1 labeling index (LI), loss of heterozygosity on the chromosome 10 (LOH10), and the epidermal growth factor receptor gene amplification (*EGFR* amplification) were analyzed.[3,4,21] An immunohistochemical analysis (IHC) was carried out on CNS

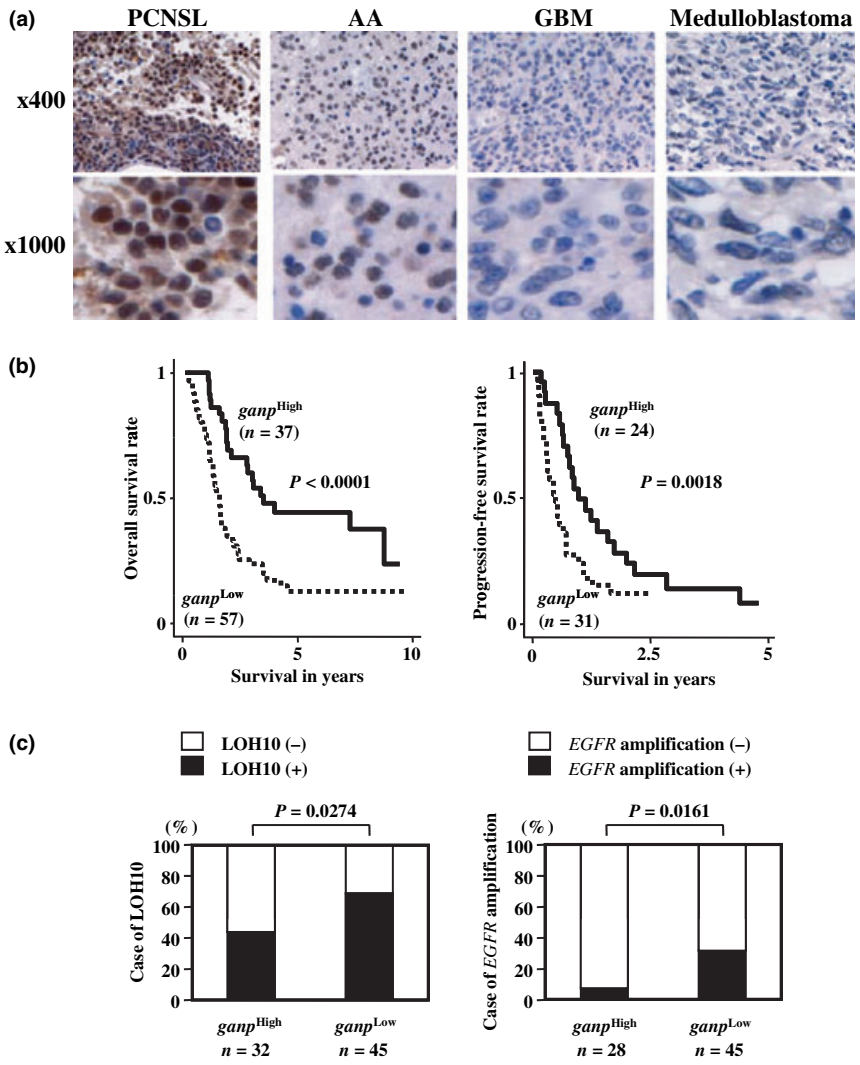

Fig. 1. Germinal center–associated nuclear protein (GANP) expression in central nervous system (CNS) tumors. (a, upper panel) GANP expression in various CNS tumors by immunohistochemistry (IHC). Original magnification ×400 for each panel. (lower panel) The larger magnification of images is shown (×1000). (b, left panel) Comparison of overall survival of malignant gliomas (MGs) between the cases of either high or low *ganp* mRNA expression using the Kaplan–Meier method. The patient group of low *ganp* mRNA expression (5 ± 6) (*ganp*^{Low}) showed a worse prognosis than the group of high expression (20 ± 11) (*ganp*^{High}) (log-rank [Mantel–Cox] test, $P < 0.0001$). (right panel) Statistical analysis of the different progression-free survivals between *ganp*^{Low} and *ganp*^{High} patients using the Kaplan–Meier method. The patients of *ganp*^{Low} (5 ± 2) showed a worse prognosis than those with *ganp*^{High} (19 ± 9) (log-rank [Mantel–Cox] test, $P = 0.0018$). (c) Comparison of other genetic abnormalities between *ganp*^{Low} and *ganp*^{High} patients. Loss of heterozygosity on the chromosome 10 (LOH10) and epidermal growth factor receptor (*EGFR*) amplification were reported[3,4] and the percentage of their positive cases is shown.

doi: 10.1111/j.1349-7006.2009.01293.x

Table 2. Comparison of GANP expression in various CNS tumors by IHC

Samples	No. of cases	GANP expression†			
		−	±	+	++
PCNSL	25	1	6	4	14
AA	10	1	4	4	1
GBM	20	3	**11**	6	0
Medulloblastoma	4	3	0	1	0

†Relative expression level of germinal center–associated nuclear protein (GANP) by immunohistochemical (IHC) score. AA, anaplastic astrocytoma; CNS, central nervous system; GBM, glioblastoma multiforme; PCNSL, primary central nervous system lymphoma.

tumor specimens. Paraffin sections (4-μm) were immunostained with rat antimouse GANP monoclonal antibody (mAb)[13] in combination with biotinylated antirat IgG Ab with Vectastain ABC complex (Vector Laboratories, Burlingame, CA, USA) and 3,3-diaminobenzidine (Sigma-Aldrich, St. Louis, MO, USA). The staining intensity was evaluated by two investigators as IHC score as follows: −, negative; ±, weak; +, intermediate; ++, strong.

Real-time RT-PCR. PCR was performed using a LightCycler (Roche Molecular Biochemicals, Indianapolis, IN, USA). Specific oligonucleotide primers and probes for *ganp* and glyceraldehyde-3-phosphate dehydrogenase (*gapdh*) were purchased (Nihon Gene Research Laboratories, Sendai, Japan). The level of *ganp* mRNA expression is determined in comparison with that of *gapdh*. Primers and probes are listed in Table 1.

Cell culture, transfection, and irradiation (IR). MRC-5 and five human MG cell lines, U251MG, U373MG, T98G, U87MG, and A172, were maintained in DMEM (Invitrogen, Carlsbad, CA, USA) supplemented with 10% fetal calf serum (Sigma-Aldrich), 2 mM L-glutamine (Cambrex, East Rutherford, NJ, USA), and 5×10^{-5} M 2-mercaptoethanol with 5% CO_2 at 37°C. Cells were transfected with 10 nM (final concentration) of the small interfering RNA (siRNA) using Lipofectamine RNAiMAX (Invitrogen). Stealth RNAi duplexes (Invitrogen) are listed in Table 1. Exposure to IR was done using Gamma-cell 40 extracter (Nordion International, Ottawa, ON, Canada) with a ^{137}Cs source.

Cell-cycle analysis. The siRNA-treated cells were collected, washed with PBS, and incubated with propidium iodide (PI) solution.[18] For bromodeoxyuridine (BrdU) incorporation analysis, siRNA-treated cells were labeled with 10 μM BrdU before harvest. DNA was stained with 7-amino-actinomycin D and fluorescein isothiocyanate (FITC)-conjugated anti-BrdU Ab using the FITC BrdU Flow Kit (BD Biosciences, San Jose, CA, USA). The cell cycle was analyzed using FACSCalibur (BD, Franklin Lakes, NJ, USA) with the CellQuest software.

Senescence-associated β-galactosidase (SA-β-gal) staining. SA-β-gal activity was detected with a Senescence β-Galactosidase Staining Kit (Cell Signaling, Danvers, MA, USA).

Immunoblotting and immunofluorescence. Cells were treated with siRNA or irradiation and lysed by TNE buffer and the cell lysates were separated by SDS-PAGE followed by immunoblotting.[13] Primary Abs against GANP,[13] p53 (Calbiochem, San Diego, CA, USA), p16 (BD Biosciences), p21 (Santa Cruz Biotechnology, Santa Cruz, CA, USA), and Rb (BD Biosciences) were used in comparison with β-actin Ab (a loading control). Cells were fixed with 3.7% paraformaldehyde and incubated with anti-trimethyl-Histone H3 (Lys9) Ab (Millipore, Bedford, MA, USA) and Alexa488-conjugated goat antirabbit IgG (Invitrogen).[18] To detect the nuclei, cells were fixed with 3.7% paraformaldehyde, permeabilized by 0.2% Triton X-100, and stained with PI.

Table 3. Comparison of *ganp* mRNA expression with clinicopathologic features in MGs

Factor	No. of cases	*Ganp* mRNA (Mean ± SD)	Mann–Whitney *U*-test *P*-values
Age (years)			
>50	58	8 ± 7	0.0020*
≤50	43	15 ± 12	
Sex			
Male	58	11 ± 9	0.8260
Female	43	12 ± 12	
Histological type			
AA (WHO grade III)**	29	19 ± 13	<0.0001*
GBM (WHO grade IV)	72	8 ± 6	
Preop KPS Score (%)			
>70	87	11 ± 10	0.5946
≤70	14	11 ± 14	
MIB-1 LI (%)			
>20	35	9 ± 8	0.0019*
≤20	66	14 ± 12	
Non-tumor brain	4	15 ± 3	n.d.

*The statistical significances are shown. **AA was selected from World Health Organization (WHO) grade III in this comparison. AA, anaplastic astrocytoma; GBM, glioblastoma multiforme; LI, labeling index; MGs, malignant gliomas; n.d., not determined; preop KPS score, preoperative Karnofsky Performance Scale score; SD, standard deviation.

Table 4. Multivariate analyses of prognostic factors in MGs

Factor	OS		PFS	
	HR (95% CI)	*P*-values	HR (95% CI)	*P*-values
Age (>50/≤50)	0.36 (0.20–0.64)	<0.01*	1.01 (0.48–2.10)	0.98
WHO grade (III/IV)	10.74 (3.99–28.94)	<0.01*	2.51(1.18–5.31)	0.01*
MIB-1 LI (>20/≤20)	1.16 (0.71–1.91)	0.54	0.63 (0.32–1.27)	0.19
ganp expression (≥10/<10)	1.02 (0.56–1.84)	0.95	0.48 (0.22–1.05)	0.06

*The statistical significances are shown. CI, confidence interval; *ganp*, germinal center–associated nuclear protein; HR, hazard ratio; LI, labeling index; MGs, malignant gliomas; WHO, World Health Organization.

Fluorescence *in situ* hybridization (FISH). U251MG cells treated with siRNA were incubated with colcemid (0.02 μg/mL) for 4 h, harvested, re-suspended in 0.075 M KCl, and fixed in 3:1 methanol/glacial acetic acid. The centromeric region-specific FISH probes for human chromosomes were prepared using two bacterial artificial chromosomes RP11-88E13 and RP11-164B7 by labeling with digoxigenin-11-dUTP (for chromosome 7) and dinitrophenyl-11-dUTP (for chromosome 9), respectively. Cells were incubated with the mixed probes with Cy3-labeled anti-digoxigenin and Cy5-labeled anti-dinitrophenyl Abs in comparison with 4′,6-diamino-2-phenylindole staining. The images were captured with the CW4000 FISH application program (Leica Microsystems Imaging Solution, Cambridge, UK).

Statistical analyses. The non-parametric Mann–Whitney *U*-test was adopted for statistical analysis of the association between *ganp* mRNA expression and clinicopathologic factors. Overall survival (OS) and progression-free survival (PFS) curves were prepared by Kaplan–Meier method and verified by the log-rank (Mantel–Cox) test. The independent effect of each parameter on OS and PFS was analyzed using the multivariate Cox proportional hazards regression model. The difference was considered significant when a *P*-value of <5% was obtained.

Results

Decreased expression of GANP in MGs. GANP expression occurs at high levels in various human hematological disorders including Hodgkin's lymphoma, acute myeloid leukemia, and myelodysplastic syndrome.[18] *Ganp*-Tg mice develop Hodgkin-like lymphomas at high incidence, which confirmed the association between increased GANP expression and tumorigenesis.[18] Here, we examined the expression of GANP in various CNS tumors by using IHC (Fig. 1a, Table 2). GANP was expressed at high levels in primary CNS lymphomas (PCNSL), but at rather lower ones in the malignant tumors of AA, GBM, and medulloblastoma. The larger magnification images were shown in the lower panel. Thus, we examined the expression of *ganp* mRNA in 101 cases of MGs (29 cases of AA and 72 cases of GBM) and four cases of non-tumor brain by quantitative real-time RT-PCR as the relative copy number in comparison with the control *gapdh* mRNA (Table 3). The non-tumor brain tissues showed the expression of *ganp* mRNA at 15 copies in the average. In MGs, the *ganp* mRNA was at seven copies as the median value (between 0 and 58 copies). The cases were divided into two groups by age (≤50 years and >50 years), sex, the histological type of AA and GBM corresponding to World Health Organization (WHO) grade III and IV, respectively, preoperative Karnofsky Performance Scale (KPS) score (<70 and ≥70), or MIB-1 LI (<20 and ≥20). The expression of *ganp* mRNA did not show any significant difference in the comparison by sex or preoperative KPS score; however, it differed significantly in the comparison by age, WHO grade, or MIB-1 LI. The level of *ganp* mRNA was significantly lower in the case of patients >50 years of age, GBM (WHO grade IV), or high MIB-1 LI; and the difference was marked in the comparison by WHO grade. The GBM group showed significantly lower expression of *ganp* mRNA (8 ± 6) than AA (grade III; 19 ± 13; $P < 0.0001$). This observation suggests that decreased expression of *ganp* mRNA might be associated with the malignant character of tumors.

A clinically meaningful cut-off point for *ganp* mRNA expression was determined for the comparison between the expression and the post-operative survival time by using the Kaplan–Meier method and log-rank (Mantel–Cox) test. A remarkable difference was observed when the cases were compared at the cut-off point of 10 copies, with the cases being classified into $ganp^{Low}$ (<10) and $ganp^{High}$ (≥10) groups. The $ganp^{Low}$ patient group showed significantly worse survival than the $ganp^{High}$ group in terms of the OS rate ($P < 0.0001$) and in terms of the PFS rate ($P = 0.0018$, Fig. 1b). To assess the association of survival duration with multiple clinical characteristics (age, WHO grade, MIB-1 LI, and *ganp* mRNA expression), we performed multivariate analysis (Table 4). Age and WHO grade were found to be independent prognostic factors for OS, but the decrease of *ganp* mRNA expression was not an independent prognostic factor for OS and PFS.

Association of LOH10 and *EGFR* amplification with the decreased expression of GANP in MGs. To investigate further the relevance of low *ganp* expression to the development of gliomas, we compared the existence of LOH10[3] and *EGFR* amplification[4] between the $ganp^{Low}$ and the $ganp^{High}$ glioma groups. LOH10 appeared in 69% of $ganp^{Low}$ cases, which was much higher ($P = 0.0274$) than the 44% for the $ganp^{High}$ cases (Fig. 1c, *left*). *EGFR* amplification was detected in 31% of $ganp^{Low}$ cases, which was four times higher ($P = 0.0161$) than the 7% for the $ganp^{High}$ ones (Fig. 1c, right). The decrease in *ganp* mRNA expression thus appears to be an indicator of the poor prognosis of MGs.

Effect of decreased GANP expression on cell proliferation and cell-cycle progression of human diploid fibroblast cells. To examine whether a decrease in GANP expression causes abnormal cell growth, we treated human diploid fibroblast MRC-5 cells with a siRNA for *ganp*. The *ganp* siRNA markedly suppressed the expression of *ganp* transcripts compared with the control siRNA as assessed by real-time RT-PCR (Fig. 2a, left) and this suppression was confirmed by immunoblotting (Fig. 2a, right). Next, the cells were examined by cell-cycle analysis after BrdU incorporation (Fig. 2b). Treatment with *ganp* siRNA caused remarkable cell-cycle abnormalities after 2 days, i.e., an increase in the number of mitotic cells and a decrease in that of S-phase cells, and no alteration in that of apoptotic cells, as determined by flow cytometric analysis (Fig. 2b). Another set of *ganp* siRNA (*ganp* siRNA2) also suppressed *ganp* expression and caused the similar cell-cycle change, indicating that the cell-cycle change was really induced by the suppression of GANP (Fig. 2c). *Ganp* RNA interference (RNAi)-treatment of MRC-5 cells caused a marked increase in the number of SA-β-gal$^+$ cells compared with that obtained with control siRNA-treated cells (Fig. 2d). MRC-5 cells showed the cell-cycle arrest of the cellular-senescence phenotype after *ganp* RNAi-treatment. Cellular senescence induced after *ganp* RNAi-treatment was caused by prolonged cell-cycle arrest with activation of p16 and the decrease of Rb expression similar to those caused by 6-Gy irradiation (Fig. 2b,e). We confirmed that cellular senescence had occurred in *ganp* siRNA-treated cells, by analyzing senescence-associated heterochromatin foci (SAHF) as another feature of cellular senescence.[22] K9M-H3, a marker of SAHF[22], appeared as typical punctate regions of DNA corresponding to heterochromatic foci in *ganp* siRNA-treated cells (Fig. 2f).

Effect of decreased GANP expression in MG cell lines harboring genetic abnormalities. Five MG cell lines (Table 4), U251MG, U373MG, U87MG, T98G, and A172, carrying various genetic abnormalities showed cell-cycle abnormalities with various degrees of hyperploidy after anti-microtubule drug (AMD) treatment.[23–25] In contrast with the case of MRC-5 fibroblasts, *ganp* RNAi-treatment caused remarkable cell-cycle abnormalities in U251MG cells, with an increase in the percentage of mitotic cells (from 15.2% to 23.3%) and hyperploid cells (from 1.36% to 15.6%) at day 5, as determined by flow cytometric analysis (Fig. 3a, left). On the contrary, U87MG cells showed no significant change in the generation of hyperploid cells (from 5.08% to 6.41%) after the same treatment; whereas G2/M-phase cells increased (from 25.2% to 31.9%; Fig. 3a, right). This result indicates that *ganp* RNAi-treatment caused the hyperploidy in U251MG in a cell-type specific manner. A peculiar difference between U251MG and U87MG cells is the p53 state. U251MG carries a *p53* mutation, whereas U87MG has the wild-type (WT) *p53*.[23] Immunoblot analysis showed that the level of WT p53 was increased in *ganp* siRNA-treated U87MG, indicating that the cell-cycle checkpoint governed by p53 operated normally in this cell line (Fig. 3b). The mutant p53 might allow the mitotic slippage of U251MG cells undergoing DDR.[24] U87MG and A172 carrying WT p53 did not show any increase in the percentage of hyperploid cells; whereas the other cell lines carrying p53 mutations, U251MG, U373MG, and T98G, generated more hyperploid cells (Table 5).

Induction of CIN by *ganp* RNAi-treatment in MG cell lines that harbor p53 mutations. *Ganp* RNAi-treatment generated large nuclei with abnormal contours in U251MG cells but not in U87MG ones, as detected by PI staining (Fig. 3c, arrows). We further examined whether *ganp* RNAi-treatment would cause increases in CIN and the number of *EGFR* genes as in glioma cells.[26–30] The hyperploidy was examined by using FISH to detect the multiplicity of chromosome 7 carrying the *EGFR* gene and chromosome 9 (Fig. 3d). Typically in control siRNA-treated U251MG cells, there were more than two copies of chromosome 7 (red);[24] however, *ganp* RNAi-treatment increased the number of chromosomes to over 10 signals per cell (Fig. 3). These results indicate that the decrease in the level of *ganp* mRNA resulted in cell-cycle abnormali-

doi: 10.1111/j.1349-7006.2009.01293.x

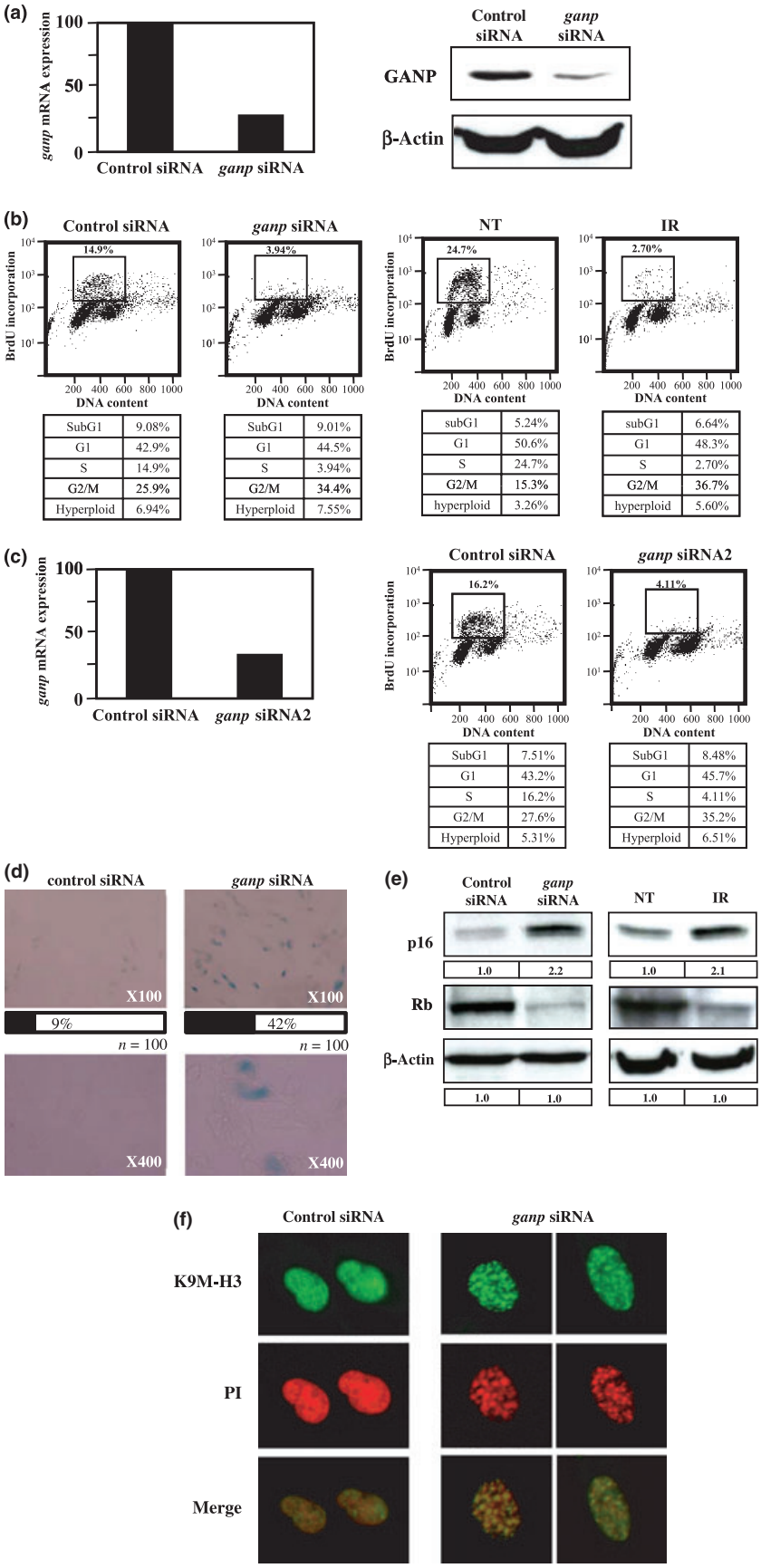

Fig. 2. Induction of cellular senescence by germinal center–associated nuclear protein (*ganp*) RNA interference (RNAi)-treatment in human diploid fibroblast. (a, left panel) Suppression of GANP by *ganp* RNAi-treatment. *Ganp* mRNA was examined by real-time PCR in siRNA-treated MRC-5 after 48 h. *Ganp* mRNA is shown as the arbitrary copy in comparison with *gapdh* mRNA. (right panel) GANP protein was examined by immunoblot analysis. β-Actin was used as a loading control. (b) Effect of RNAi-treatment or irradiation (IR) on MRC-5 was examined by cell-cycle analysis. Cell-cycle distribution was examined by BrdU incorporation on the *x*-axis with the total DNA content on the *y*-axis. Box indicates cells in the S-phase. (c, left panel) Another sequence of *ganp* RNAi-treatment (*ganp* siRNA2) in human diploid fibroblast. Suppression of *ganp* transcription in *ganp* siRNA2-treated cells. *Ganp* mRNA was examined by real-time PCR in *ganp* siRNA2-treated MRC-5 after 48 h. *Ganp* mRNA is shown as the arbitrary copy in comparison with *gapdh* mRNA. (right panel) Cell-cycle analysis in *ganp* siRNA2-treated cells. Cell-cycle distribution was examined by BrdU incorporation on the *x*-axis with the total DNA content on the *y*-axis. Box indicates cells in the S-phase. (d) Induction of SA-β-gal activity in MRC-5 after *ganp* RNAi-treatment. Images of low (×100) and high (×400) magnification are shown in control or *ganp* siRNA-treated cells. Percentages indicate the number of SA-β-gal$^+$ cells per 100 cells. (e) Expression of cell cycle–related molecules in MRC-5 after *ganp* RNAi- or IR-treatment. Cell lysates from MRC-5 treated with siRNA or IR were subjected to immunoblotting with the Abs. (f) Induction of SAHF in MRC-5 after *ganp* RNAi-treatment. MRC-5 were stained with anti-trimethyl-Histone H3 (Lys9) (K9M-H3) Ab and viewed under a fluorescent microscope. Counterstaining was done by propidium iodine (PI).

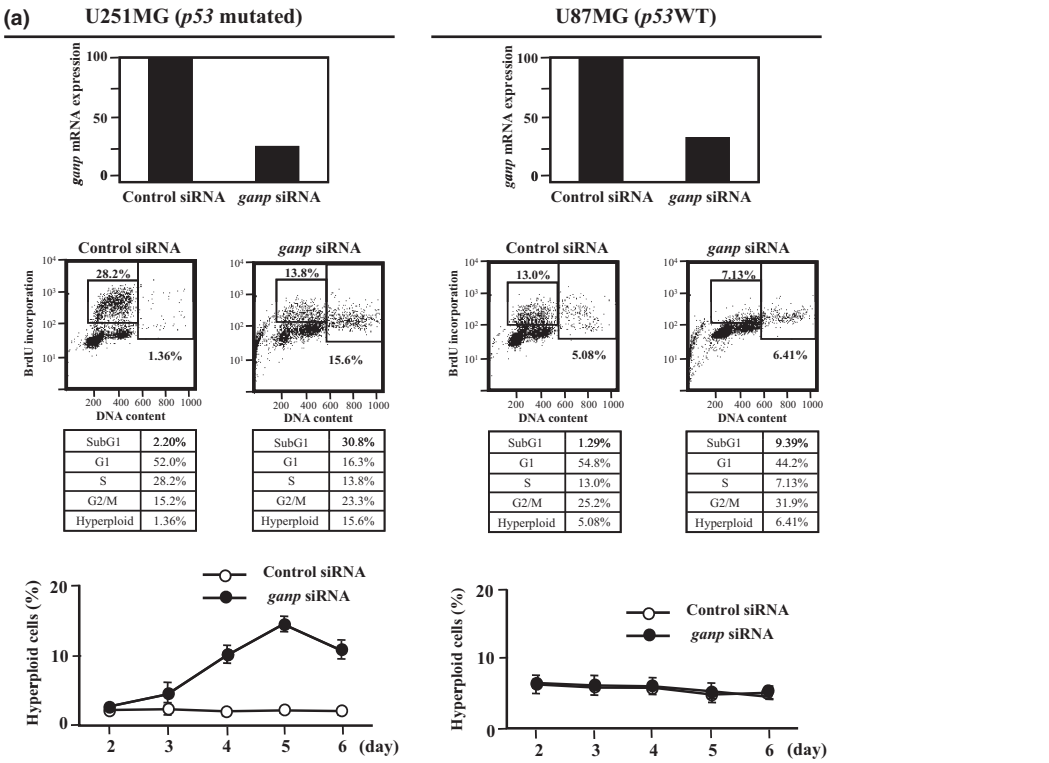

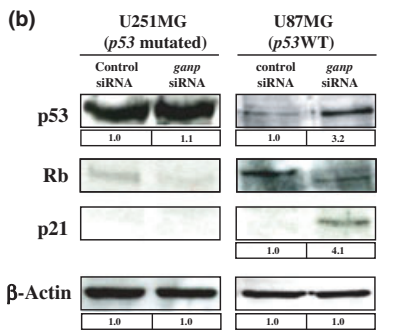

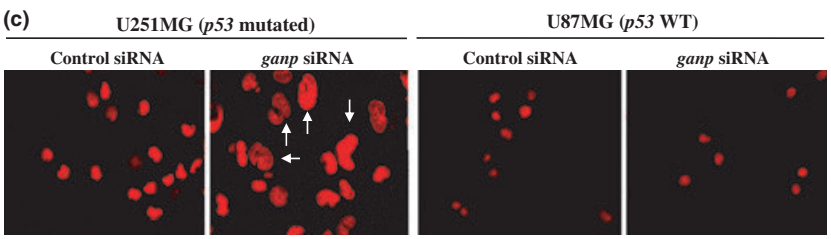

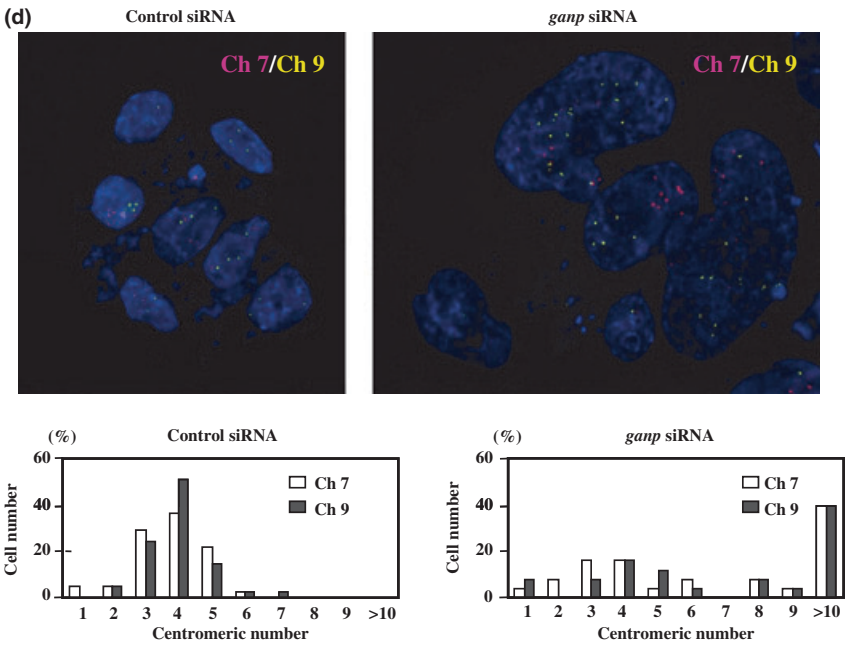

doi: 10.1111/j.1349-7006.2009.01293.x

Table 5. Effect of *ganp* siRNA on various malignant glioma cell lines

Cell line	Gene state†		Hyperploid cell (%)‡	
	p53	*p16*	Control siRNA	*ganp* siRNA
U251MG	Mutated	Deleted	1.84 ± 0.23	16.5 ± 0.85
U87MG	WT	Deleted	4.57 ± 0.69	5.43 ± 1.08
U373MG	Mutated	Deleted	1.58 ± 0.08	17.2 ± 1.05
T98G	Mutated	Deleted	2.40 ± 0.31	21.0 ± 0.53
A172	WT	Deleted	1.91 ± 0.59	1.13 ± 0.11

†Gene states were obtained from a previous report.[43] ‡Hyperploid cells were calculated by flow cytometry after 5 days of RNA interference (RNAi)-treatment. *ganp*, germinal center–associated nuclear protein.

ties generating hyperploid cells, in association with another genetic abnormality (in this case, the p53 mutation) of cell-cycle control.

Discussion

In this study, we focused on the expression of GANP in MGs with a poor prognosis and studied the molecular mechanism to explain how the low *ganp* expression is associated with the generation of CIN in MG cell lines. Our results demonstrated that the expression of GANP, a putative component of the ribonucleoprotein complex, is significantly decreased in the group of MGs with poor prognosis.

The formation of mature ribonucleoprotein particles probably plays a role not only in gene expression, but also in the maintenance of genome stability.[31] Null mutation of any component of suppressor of the Transcriptional defects of Hpr1Δ by Overexpression (THO) results in similar phenotypes of transcription impairment and defects in mRNA export. Analysis of THO mutants in yeast led to the hypothesis that transcription-associated hyper-recombination is tightly linked to transcriptional-elongation impairment and is presumably caused by the co-transcriptional formation of R-loops (DNA–RNA hybrids).[32]

We examined how the decrease in the GANP level affected cell-cycle progression and generated hyperploidy in MG cell lines of different genetic abnormalities; and based on our results we propose a model to show how GANP insufficiency is associated with malignant progression of MGs (Fig. 4). The lack of p53 results not only in the DNA damage-induced impairment of checkpoints but also in the impairment of the spindle assembly checkpoint, and cells lacking p53 become hyperploid after treatment with AMD.[33,34] GANP insufficiency causes cells to initiate DDR. When the DNA damage is irreparable, cells undergo apoptosis or cellular senescence (Fig. 4a). However, MG cells harboring various genetic abnormalities may become hyperploid by the decreased expression of GANP under the G1-checkpoint abrogation that leads to the continuation of cell cycling as mitotic slippage (Fig. 4b). The MG cell lines harboring WT p53 did not generate hyperploid cells by inhibiting cell-cycle progression at the G2/M-phase after the DDR, suggesting that the critical gatekeeper is p53 in the transcription-coupled DDR.

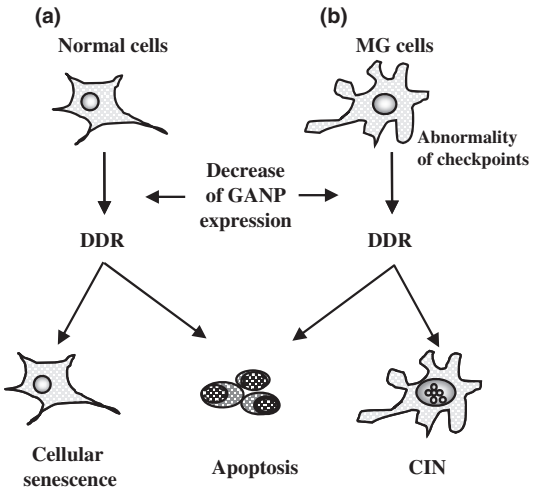

Fig. 4. A proposed model regarding germinal center–associated nuclear protein (GANP) insufficiency and malignant progression of malignant gliomas (MGs). GANP insufficiency causes normal or malignant cells to initiate DNA damage response (DDR). In case of irreparable DNA damages, normally cells cause apoptosis or cellular senescence accompanied with up-regulation of p16 (a). Adversely, MG cells harboring various genetic abnormalities including p53 mutation may generate hyperploid cells by GANP insufficiency under the G1-checkpoint abrogation that leads to the continuation of cell cycling as mitotic slippage (b).

Cells with DNA damage normally undergo cell-cycle arrest at the G2-phase, owing to the intact G2 checkpoint. These cells undergo cellular senescence without further progression of the cell cycle. GANP insufficiency causes a continuous cell-cycle arrest and generates cellular-senescence changes, although it may not be a direct cause of oncogenesis under the intact checkpoint regulation.

The senescence response appears to be due to either one or both of the two pathways leading to senescent cell-cycle arrest, which are governed by tumor suppressor proteins p53 and Rb.[35,36] The inhibitor of CDKs (INK) proteins including $p16^{INK4a}$ specifically inhibit the activity of cyclin D-dependent kinases to prevent the phosphorylation of Rb family proteins.[37,38] The $p16^{INK4a}$-Rb pathway controls the cell cycle at the G1-phase and induces cell-cycle arrest as replicative senescent cells, which are represented by the development of dense foci of heterochromatin.[22,39] Treatment with *ganp* siRNA markedly augmented the expression of p16 and prevented the phosphorylation of Rb, indicating that the DDR caused by GANP insufficiency was mediated by the $p16^{INK4a}$-Rb pathway.

The transcription of the *ganp* gene is regulated by the E2F consensus element (at -56 bp in the mouse).[40] The E2F transcription factor plays a pivotal role in the timely activation of gene expression during mammalian cell-cycle progression.[41] Co-expression of E2F-2 and p53 enhances the anti-cancer effect of p53 in glioma cells.[42] The critical elements associated with

Fig. 3. Induction of hyperploid cells by germinal center–associated nuclear protein (*ganp*) RNA interference (RNAi -treatment in human malignant glioma (MG)cell lines. (a, upper panel) Suppression of *ganp* transcription by *ganp* RNAi-treatment. *Ganp* mRNA was examined by real-time RT-PCR in U251MG and U87MG after 48 h of RNAi-treatment. *Ganp* mRNA is shown as the arbitrary copy in comparison with *gapdh* mRNA. (middle panel) Effect of RNAi-treatment on U251MG and U87MG was examined by cell-cycle analysis after 5 days. Cell-cycle distribution was examined by BrdU incorporation on the *x*-axis and total DNA content on the *y*-axis. Left box, cells in the S-phase; right box, cells in hyperploid cells with DNA content larger than 4N. (lower panel) Line graphs summarizing the percentage of hyperploid cells with more than 4N DNA content were measured over a 6-day period using two cell lines. (b) Expression of cell cycle–related molecules in MG cell lines after *ganp* RNAi-treatment. Cell lysates from U251MG and U87MG treated with siRNA were subjected to immunoblotting with Abs. (c) DNA staining of U251MG and U87MG was performed after RNAi-treatment. Arrows indicate large nucleated cells in comparison with control siRNA-treated cells (magnification, ×400). (d, upper panel) Dual-color FISH analysis of U251MG after RNAi-treatment. U251MG treated with siRNA were examined after 5 days by FISH using fluorescent probes for chromosome 7 (red) and 9 (yellow) (magnification, ×1000). (lower panel) The centromeric copy number was scored by examining more than 50 cells.

tumorigenesis and malignant progression of MG cases need to be determined.

In conclusion, we have herein shown that down-regulation of GANP caused cellular senescence in fibroblast cells and also caused CIN in association with a p53 abnormality in MGs.

Acknowledgments

This work was supported by Grant-in-Aid from the Ministry of Education, Culture, Sports, Science and Technology of Japan; CREST of JST; and the Advanced Education Program for Integrated Clinical, Basic and Social Medicine, Graduate School of Medical Sciences, Kumamoto University. We thank Dr. Masahisa Tsuji for dual-color FISH and Ms. Masako Obata for technical assistance.

Disclosure Statement

There is no conflict of interest for any of the authors.

References

1 Zhu Y, Parada LE. The molecular and genetic basis of neurological tumours. *Nat Rev Cancer* 2002; **2**: 616–26.
2 The Cancer Genome Atlas Research Network. Comprehensive genomic characterization defines human glioblastoma genes and core pathways. *Nature* 2008; **455**: 1061–8.
3 Tada K, Shiraishi S, Kamiryo T *et al.* Analysis of loss of heterozygosity on chromosome 10 in patients with malignant astrocytic tumors: correlation with patient age and survival. *J Neurosurg* 2001; **95**: 651–9.
4 Shinojima N, Tada K, Shiraishi S *et al.* Prognostic value of epidermal growth factor receptor in patients with glioblastoma multiforme. *Cancer Res* 2003; **63**: 6962–70.
5 Reifenberger G, Liu L, Ichimura K, Schmidt EE, Collins VP. Amplification and overexpression of the MDM2 gene in a subset of human malignant gliomas without *p53* mutations. *Cancer Res* 1993; **53**: 2736–9.
6 Albertson DG, Collins C, McCormick F, Gray JW. Chromosome aberrations in solid tumors. *Nat Genet* 2003; **34**: 369–76.
7 Di Micco R, Fumagalli M, d'Adda di Fagagna F. Breaking news: high-speed race ends in arrest – how oncogenes induce senescence. *Trends Cell Biol* 2007; **17**: 529–36.
8 Svejstrup JQ. Mechanisms of transcription-coupled DNA repair. *Nat Rev Mol Cell Biol* 2002; **3**: 21–9.
9 Gaillard H, Wellinger RE, Aguilera A. A new connection of mRNP biogenesis and export with transcription-coupled repair. *Nucleic Acids Res* 2007; **35**: 3893–906.
10 Fischer T, Strasser K, Racz A *et al.* The mRNA export machinery requires the novel Sac3p-Thp1p complex to dock at the nucleoplasmic entrance of the nuclear pores. *EMBO J* 2002; **21**: 5843–52.
11 Gallardo M, Luna R, Erdjument-Bromage H, Tempst P, Aguilera A. Nab2p and the Thp1p-Sac3p complex functionally interact at the interface between transcription and mRNA metabolism. *J Biol Chem* 2003; **278**: 24225–32.
12 Aguilera A. Cotranscriptional mRNP assembly: from the DNA to the nuclear pore. *Curr Opin Cell Biol* 2005; **17**: 242–50.
13 Kuwahara K, Yoshida M, Kondo E *et al.* A novel nuclear phosphoprotein, GANP, is up-regulated in centrocytes of the germinal center and associated with MCM3, a protein essential for DNA replication. *Blood* 2000; **95**: 2321–8.
14 Kuwahara K, Fujimura S, Takahashi Y *et al.* Germinal center-associated nuclear protein contributes to affinity maturation of B cell antigen receptor in T cell-dependent responses. *Proc Natl Acad Sci USA* 2004; **101**: 1010–5.
15 Sakaguchi N, Kimura T, Matsushita S *et al.* Generation of high-affinity antibody against T cell-dependent antigen in the *ganp* gene-transgenic mouse. *J Immunol* 2005; **174**: 4485–94.
16 Kuwahara K, Tomiyasu S, Fujimura S *et al.* Germinal center-associated nuclear protein (GANP) has a phosphorylation-dependent DNA primase activity that is up-regulated in germinal center regions. *Proc Natl Acad Sci USA* 2001; **98**: 10279–83.
17 Takei Y, Swietlik M, Tanoue A, Tsujimoto G, Kouzarides T, Laskey R. MCM3AP, a novel acetyltransferase that acetylates replication protein MCM3. *EMBO Rep* 2001; **2**: 119–23.
18 Fujimura S, Xing Y, Takeya M *et al.* Increased expression of germinal center-associated nuclear protein RNA-primase is associated with lymphomagenesis. *Cancer Res* 2005; **65**: 5925–34.
19 Yoshida M, Kuwahara K, Shimasaki T, Nakagata N, Matsuoka M, Sakaguchi N. GANP suppresses DNA recombination, measured by direct-repeat β-*galactosidase* gene construct, but does not suppress the type of recombination applying to immmunoglobulin genes in mammalian cells. *Genes Cells* 2007; **12**: 1205–13.
20 Shiraishi S, Tada K, Nakamura H *et al.* Influence of p53 mutations on prognosis of patients with glioblastoma. *Cancer* 2002; **95**: 249–57.
21 Kamiryo T, Tada K, Shiraishi S *et al.* Analysis of loss of homozygous deletion of the p16 gene and correlation with survival in patients with glioblastoma multiforme. *J Neurosurg* 2002; **96**: 815–22.
22 Narita M, Nunez S, Heard E *et al.* Rb-mediated heterochromatin formation and silencing of E2F target genes during cellular senescence. *Cell* 2003; **113**: 703–16.
23 Nitta M, Tsuiki H, Arima Y *et al.* Hyperploidy induced by drugs that inhibit formation of microtubule promotes chromosome instability. *Genes Cells* 2002; **7**: 151–62.
24 Tsuiki H, Nitta M, Tada M *et al.* Mechanism of hyperploid cell formation induced by microtubule inhibiting drug in glioma cell lines. *Oncogene* 2001; **20**: 420–9.
25 Hong FD, Chen J, Donovan S *et al.* Taxol, vincristine or nocodazole induces lethality in G1-checkpoint-defective human astrocytoma U373MG cells by triggering hyperploid progression. *Carcinogenesis* 1999; **20**: 1161–8.
26 Nishizaki T, Harada K, Kubota H *et al.* Chromosomal instability in malignant astrocytic tumors detected by fluorescence *in situ* hybridization. *J Neurooncol* 2002; **56**: 159–65.
27 Nishizaki T, Kubota H, Harada K *et al.* Clinical evidence of distinct subgroups of astrocytic tumors defined by comparative genomic hybridization. *Hum Pathol* 2000; **31**: 608–14.
28 Lengauer C, Kinzler KW, Vogelstein B. Genetic instabilities in human cancers. *Nature* 1998; **396**: 643–9.
29 Saito T, Hama S, Izumi H *et al.* Centrosome amplification induced by survivin suppression enhances both chromosome instability and radiosensitivity. *Br J Cancer* 2008; **98**: 345–55.
30 Inoue T, Hiratsuka M, Osaki M *et al.* SIRT2, a tubulin deacetylase, acts to block the entry to chromosome condensation in response to mitotic stress. *Oncogene* 2007; **26**: 945–57.
31 Luna R, Jimeno S, Marín M, Huertas P, García-Rubio M, Aguilera A. Interdependence between transcription and mRNP processing and export, and its impact on genetic stability. *Mol Cell* 2005; **18**: 711–22.
32 Huertas P, Aguilera A. Cotranscriptionally formed DNA:RNA hybrids mediate transcription elongation impairment and transcription-associated recombination. *Mol Cell* 2003; **12**: 711–21.
33 Di Leonardo A, Khan SH, Linke SP *et al.* DNA rereplication in the presence of mitotic spindle inhibitors in human and mouse fibroblasts lacking either p53 or pRb function. *Cancer Res* 1997; **57**: 1013–9.
34 Khan SH, Wahl GM. p53 and pRb prevent rereplication in response to microtubule inhibitors by mediating a reversible G1 arrest. *Cancer Res* 1998; **58**: 396–401.
35 Finkel T, Serrano M, Blasco MA. The common biology of cancer and aging. *Nature* 2007; **448**: 767–74.
36 Mooi WJ, Peeper DS. Oncogene-induced cell senescence-halting on the road to cancer. *N Engl J Med* 2006; **355**: 1037–46.
37 Ruas M, Peters G. The p16INK4a/CDKN2A tumor suppressor and its relatives. *Biochim Biophys Acta* 1998; **1378**: F115–77.
38 Sherr CJ, Roberts JM. CDK inhibitors: positive and negative regulators of G1-phase progression. *Genes Dev* 1999; **13**: 1501–12.
39 Zhang R, Poustovoitov MV, Ye X *et al.* Formation of MacroH2A-containing senescence-associated heterochromatin foci and senescence driven by ASF1a and HIRA. *Dev Cell* 2005; **8**: 19–30.
40 EL-Gazzar MA, Maeda K, Nomiyama H, Nakao M, Kuwahara K, Sakaguchi N. PU.1 is involved in the regulation of B lineage-associated and developmental stage-dependent expression of the germinal center-associated DNA primase GANP. *J Biol Chem* 2001; **276**: 48000–8.
41 Takahashi Y, Rayman JB, Dynlacht BD. Analysis of promoter binding by the E2F and pRB families in vivo: distinct E2F proteins mediate activation and progression. *Genes Dev* 2000; **14**: 804–16.
42 Mitlianga PG, Kyritsis AP, Gomez-Manzano C *et al.* Co-expression of E2F-2 enhances the p53 anti-cancer effect in human glioma cells. *Int J Oncol* 2001; **18**: 343–7.
43 Wang C-C, Liao Y-P, Mischel PS, Iwamoto KS, Cacalano NA, McBride WH. HDJ-2 as target for radiosensitization of glioblastoma multiforme cells by the farnesyltransferase inhibitor R115777 and the role of the p53/p21 pathway. *Cancer Res* 2006; **66**: 6756–62.

doi: 10.1111/j.1349-7006.2009.01293.x